# Inflamed Appendix Detection from Laparoscopic Video Footage Using Edge Detection and Morphological Image Processing


**Supervisor:** **Dr. Jia Uddin**

| | |
|---|---|
| Siddiq Husain Tashfeen | 12201037 |
| Asir Abrar | 13101288 |
| Tasmia Taslim Tondra | 12201109 |

**Department of Computer Science and Engineering**

**BRAC University**

**Submitted on: 21st August 2017**

# DECLARATION

We, hereby declare that this thesis is based on the results found by ourselves. Materials of work found by other researcher are mentioned by reference. This Thesis, neither in whole or in part, has been previously submitted for any degree.

Signature of Supervisor

Dr. Jia Uddin

Signature of Author

Siddiq Husain Tashfeen

Asir Abrar

Tasmia Taslim Tondra

# ACKNOWLEDGEMENTS

All thanks to Almighty ALLAH, the creator and the owner of this universe, the most merciful, beneficent and the most gracious, who provided us guidance, strength and abilities to complete this research.

We are especially thankful to Dr. Jia Uddin, our thesis supervisor, for his help, guidance and support in completion of our project. We also thankful to the BRAC University Faculty Staffs of the Computer Science and Engineering, who have been a light of guidance for us in the whole study period at BRAC University, particularly in building our base in education and enhancing our knowledge.

Finally, we would like to express our sincere gratefulness to our beloved parents, brothers and sisters for their love and care. We would like to thank specially to Wasif Shafaet Chowdhury for helping us and grateful to all of our friends who helped us directly or indirectly to complete our thesis.

# CONTENTS


**DECLARATIONS** ii

**ACKNWOLEDGEMENTS** iii

**CONTENTS** iv

**LIST OF FIGURES** vii

**LIST OF TABLES** viii

**ABSTRACT** 1

CHAPTER 01: INTRODUCTION

1.1 Motivations 2

1.2 Contribution Summary 2

1.3 Thesis Orientation 3

CHAPTER 02: BACKGROUND INFORMATION

2.1 Appendix 4

2.2 Alternative Techniques

2.2.1 Needlescopic laparoscopic appendectomy 7

2.2.2 Two port laparoscopic appendectomy 7

2.2.3 Appendectomy with a single, tensom biblical trocar 7

2.2.4 Single access laparoscopic appendectomy 7

2.3 Complications of laparoscopic appendectomy

2.3.1 Bleeding 8

2.3.2 Fecalith 8

2.4 Effects of Laparoscopic Appendectomy

2.4.1 Laparoscopic appendectomy in women of childbearing age 8

2.4.2 Laparoscopic appendectomy in pregnant women 8

2.4.3 Laparoscopic appendectomy in children 8

2.4.4 Laparoscopic appendectomy in obese persons 9

2.5 Edge detection 9

2.6 Canny edge detection 11
2.7 Close method 12
2.8 Image erode and dilation 12
CHAPTER 03: METHODOLOGY
3.1 Introduction 14
3.2 Work Flow 15
3.3 Pre-processing
3.3.1 RGB to Grayscale 17
3.3.2 Median Filtering 18
3.3.3 Image Binarization 19
3.4 Edge Detection
3.4.1 Canny Edge Detection 20
3.5 Morphological Image Processing
3.5.1 Close Method 22
3.5.2 Dilation and Erosion 22
3.5.3 Hole Filling 24
3.5.4 Erosion 25
3.6 Min-Max for Window Creation 26
CHAPTER 04: EXPERIMENTAL ANALYSIS
4.1 Introduction 27
4.2 Using Erosion Method Again 27
4.3 Changes in Accuracy Rate Based on Changes in the Threshold Values 28
CHAPTER 05: CONCLUSIONS AND FUTURE WORKS
5.1 Concluding Remarks 31
5.2 Future Works
5.2.1 Work for detection of other organs 31
5.2.2 Robotic Surgery 31

**REFERENCES** 32

## LIST OF FIGURES


Fig 2.1: The position of the patient, equipment and the surgical team 5
Fig 2.2: Dissection of the mesoappendix 5
Fig 2.3: Securing the base of the appendix with an endoloop 6
Fig 2.4: Securing the base of the appendix using a stapler 6
Fig 2.5: Securing the base of the appendix with a Hem-o-lok XL clip 6
Fig 2.6: One Edge Map 10
Fig 2.7: Laplacian Edge Detection 11
Fig 3.1: Work Flow 15
Fig 3.2: Image from Laparoscopic video footage for preprocessing 16
Fig 3.3: RGB to Grayscale 18
Fig 3.4: Gray scale to median filtered 19
Fig 3.5: Max and min value 21
Fig 3.6: Median filtered to canny edge detected images 22
Fig 3.7: Dilation and erosion 23
Fig 3.8: Canny edge detected image to close image 24
Fig 3.9: Close image to hole filled 25
Fig 3.10: Hole filled image mapped to RGB image 25
Fig 3.11: Eroded image to RGB image 26
Fig 3.12: Eroded image to window creation 26
Fig 4.1: Differece after first time eroding and second time eroding 27
Fig 4.2: Accuracy rate based on threshold value from 0.1 to 0.9 28
Fig 4.3: Accuracy rate based on threshold value from 0.11 to 0.19 29

## LIST OF TABLES

Table 1 – Accuracy rate based on threshold value from 0.1 to 0.9 28

Table 2 – Accuracy rate based on threshold value from .11 to .19 29

# ABSTRACT

In the world of surgical instruments laparoscopy has a vital space. Laparoscopic surgery is also called minimally invasive surgery technique where operations are performed through small incision elsewhere in the body. Laparoscopic appendectomy is one kind of surgery in which doctors perform the operation manually through small incision by looking at the monitor. In this study a new approach has been proposed, so that the machine can automatically detect the appendix, by using edge detection and morphological image processing techniques. In order to implement the proposed model a laparoscopic appendectomy video footage has been taken under consideration and every frame of the footage has been separated. After the frame separation process the proposed algorithm has been applied in every frame. It has been observed that the proposed algorithm is robust enough to detect the ROI from frames that contains noise.

# CHAPTER 01

# INTRODUCTION

## 1.1 Motivations

Inflammation of the appendix is one of the most common diseases that causes abdominal pain and requires surgical treatment. A surgical procedure to remove the appendix is performed when acute or chronic inflammation or benign tumors of the appendix are diagnosed by employing a minimally invasive laparoscopic approach which allows patients to resume daily routine activities sooner, shortens recovery time and reduces the risk of postoperative wound complications as compared with open procedures. This surgical technique is recommended for patients with overweight and those in whom the diagnosis of appendicitis is clear. To detect the inflamed appendix from laparoscopic video footage here we will use edge detection and morphological image processing technique to detect the region of interest. Using edge detection with hole filling of morphological image processing technique and by the minimum and the maximum value of the edge we detect the appendix from video footage more.

## 1.2 Contribution Summary

The summary of the main contributions is as follows:

- Edge detection has been applied to detect the edges of the interested region. To detect the edges of the region we have used the canny edge detection technique.
- After detecting the edges the close method, hole filling and erosion method have been implemented to get the accurate image of the ROI (region of interested). We have implemented these techniques to increase the difference between interested region and non interested region.
- We have bound the area where it is needed to do the operation for inflamed appendix. It has been done by finding the minimum and the maximum value of both X-axis and Y-axis of the ROI. After that the difference between the maximum and the minimum value has been measured and created a window in which the width value is equal to the difference value.

### 1.3 Thesis Orientation

The rest of the thesis is organized as follows:

- Chapter 01 includes the Motivations following contribution summary and thesis orientation
- Chapter 02 includes the necessary background information regarding the proposed approaches of appendix detection from laparoscopic video using edge detection and morphological image processing.
- Chapter 03 presents the proposed model and the methodologies.
- Chapter 04 demonstrates the experimental results and comparison.
- Chapter 05 concludes the thesis and states the future research directions.

# CHAPTER 02

# BACKGROUND INFORMATION

## 2.1 Appendix

Acute appendicitis is one of the most common causes of acute abdomen. It may occur from the time of infancy to old age, but the peak age of incidence is in the second and third decades of life. The diagnosis is based on a careful history and physical examination. In patients who have atypical clinical and laboratory findings, US, CT, MRI, a scoring system and laparoscopy can be used. Laparoscopic appendectomy is a safe and effective method for the treatment of appendicitis. It has proven advantages in relation to the open method: less post-operative pain, and a short stay in hospital, quicker recovery and return to normal activities. The causes of unsuccessful procedures vary, and most of the reasons for conversion occur due to the operator's lack of experience. In general, laparoscopic appendectomy has advantages, but it must be borne in mind that surgical experience in laparoscopic techniques is a pre-condition for surgeons to expect clinical benefits from laparoscopic appendectomy. In clinical conditions, where surgical experience is present, and the necessary equipment, the use of laparoscopy and laparoscopic appendectomy may be recommended in all patients with suspected appendicitis, if laparoscopy itself is not contra-indicated or is not feasible [1].

Laparoscopic appendectomy traditionally requires three laparoscopic ports (Figure 2.1). In all approaches, a 10 or 12 mm umbilical port is used, whilst the positions of the other ports vary. Some authors place a 5 mm trocar in the upper right quadrant and a 12 mm trocar in the lower left quadrant. However, a sub-pubic trocar position, where a 5 mm trocar is placed in the lower right quadrant (Technique 1) seems the best, with the best cosmetic effect, and especially easier manipulation of the retrocecal positioned appendix.

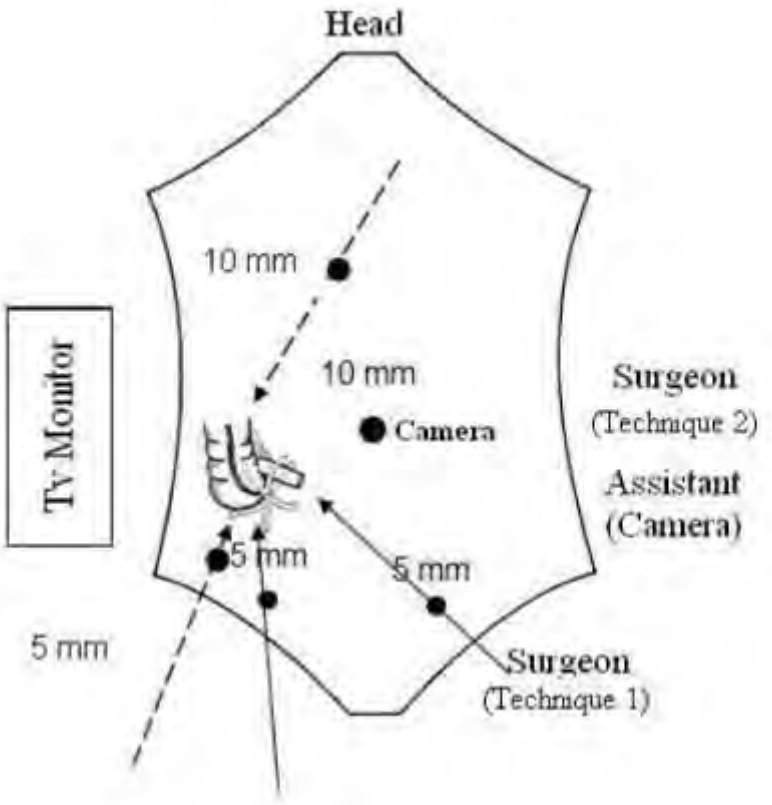


Fig 2.1: The position of the patient, equipment and the surgical team. Technique 1: The suprapubic position - a full line. Technique 2: Another position of trocars; one trocar is placed in the right upper quadrant, second one in in the lower left quadrant - dotted line. It can be seen (red arrows) that suprapubic position of trocars (Technique 1), in a retrocecal position of appendix, enables the cecum to be pushed upwards, which makes it easier to remove.

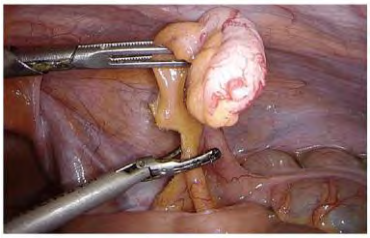

Fig 2.2: Dissection of the mesoappendix.

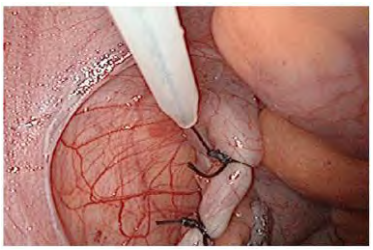

Fig 2.3: Securing the base of the appendix with an endoloop.


Fig 2.4: Securing the base of the appendix using a stapler.

Fig 2.5: Securing the base of the appendix with a Hem-o-lok XL clip.

The differences between the level of inflammation and foreign body reaction to different materials used in laparoscopic appendectomy favor the use of a stapler and plastic clips [2]. Also, the creation of adhesion in the area of the base of the appendix is lowest when a stapler is used [3]. It may be said that these characteristics of the stapler may be an advantage in taking care of the base of the appendix during laparoscopic appendectomy.

### 2.2 Alternative techniques

Alongside the classical laparoscopic appendectomy described above using three trocars, various alternative techniques have been described whose aim is to increase the benefit of the classical technique, reduce post-operative pain and have an even better cosmetic result.

### 2.2.1 Needlescopic laparoscopic appendectomy

Needlescopic instruments are defined as those of 3 mm or less in diameter, which create an even smaller trocar wound and thereby less tissue trauma [4]. The longer duration of the surgery and the larger conversion rate to open appendectomy should be emphasized at the beginning, but following the learning curve these parameters improve. It may be said that this is a feasible procedure but only in experienced hands and in selected patients, especially young girls. It is less invasive and cosmetically superior to classical appendectomy [5].

### 2.2.2 Two - port laparoscopic appendectomy

This technique includes a 12 mm infra-umbilical port and one 5 mm port in the lower left quadrant. It may be said that this technique is a transition to single port laparoscopic appendectomy [6].

### 2.2.3 Appendectomy with a single, transom bilical trocar

This is the method where the appendix, after laparoscopic dissection, is exteriorized and the appendectomy is performed externally, as in open appendectomy [7,8]. However, very often this procedure cannot be completed using only one trocar. This method in fact represents a transition to single access laparoscopic appendectomy.

### 2.2.4 Single Access Laparoscopic Appendectomy (SALA)

SALA further minimizes surgical trauma and is increasingly considered as an alternative technique to the classical laparoscopic technique. There is no difference in the degree of wound infection, the time of regulated diet, the length of hospitalization and the time of return to work between laparoscopic appendectomy and SALA [9]. But there is longer operation time, a larger dose of narcotics and hospital costs with SALA are higher. It is said that this method gives better cosmetic results than laparoscopic appendectomy. However, there is a higher degree of re-interventions in cases of complicated appendicitis treated by SALA [10].

## 2.3 Complications of laparoscopic appendectomy

Most reports of laparoscopic appendectomy indicate a low incidence of intraoperative and postoperative complications [11].

### 2.3.1 Bleeding

Bleeding is usually overestimated during laparoscopic procedures, because of the magnification of the camera [12], but most conversions to open procedure occur for this complication [13].

The major source of bleeding is placement of trocars through the central rectus muscle and laceration of inferior epigastric artery.

### 2.3.2 Fecalith

This is a rare, but frustrating complication [14]. During dissection of a distended, gangrenous appendix, a fecalith may drop into the peritoneal cavity. Retained fecaliths may cause an intrabdominal abscess. Therefore fecaliths need to be dealt with carefully and cautiously to avoid them being lost between the loops of the intestine and the pelvis. Fecatliths should be thrown into an endobag and careful lavage performed.

This complication will be found more often as laparoscopic appendectomy becomes a more common method in the treatment of acute appendicitis [14]. Surgeons should be aware of this complication in order to treat fecalith adequately when recognized intra or postoperatively.

## 2.4 Effects of Laparoscopic Appendectomy

### 2.4.1 Laparoscopic appendectomy in women of childbearing age

The incidence of misdiagnosis is between 26% and 45% in pre-menopausal women [15]. Therefore early laparoscopy potentially leads to more accurate diagnosis and reduces the risk of complications related to postponing diagnosis [15]. Other benefits are the improvement of the quality of life, pain reduction, reduction in the length of hospitalization, and the particular cosmetic effect are present as in other patients after laparoscopic appendectomy.

### 2.4.2 Laparoscopic appendectomy in pregnant women

Pregnancy is not an absolute contra-indication [16], but the increased size of the uterus reduces the working space and makes laparoscopic appendectomy more difficult.

### 2.4.3 Laparoscopic appendectomy in children

The range of acute illnesses in children is completely different than in adults but older children and adolescents are suitable candidates for laparoscopic appendectomy which has all the

benefits it has in adults, shorter hospitalization, lower levels of wound infection, quicker return to normal activities, better cosmetic effect, and better visualization of the peritoneal space.

### 2.4.4 Laparoscopic appendectomy in obese persons

Laparoscopic appendectomy is also a safe and effective method in obese persons. It has the advantage over the open approach due to the improved visualization, the reduced complications relating to the wound, but it should be pointed out that longer trocars and instruments are needed.

Laparoscopic appendicectomy though widely practiced has not gained universal approval. In India a study reflected the result of between laparoscopic appendicectomy and open appendecectomy. The study group consisted of two hundred and seventy nine patients suffering from acute appendicitis. One hundred patients underwent laparoscopic appendicectomy (LA) and one hundred seventy nine patients underwent open appendecectomy (OA). Comparison was based on length of hospital stay, operating time, postoperative morbidity, duration of convalescence and operative cost in terms of their medians. The Mann-Whitney statistics (T) were calculated and because of large samples, the normal deviate test (Z) was used [2].

Of the hundred patients, six patients (6%) had the procedure converted to open surgery. The rate of infections and overall complications (LA: 15%, OA: 31.8%, $P < 0.001$) were significantly lower in patients undergoing LA. The median length of stay was significantly shorter after LA (3 days after LA, 5 days after OA, $P < 0.0001$) than after OA. The operating time was shorter {OA: 25 min (median), LA: 28 min (median), $0.01 < P < 0.05$} in patients undergoing open appendicectomy compared to laparoscopic appendicectomy [17].

Hospital stay for LA is significantly shorter and the one-time operative charges appear to be almost the same. LA is also associated with increased clinical comfort in terms of fewer wound infections, faster recovery, earlier return to work and improved cosmesis [17].

## 2.5 Edge Detection

In 1977 Professor Ramakant Nevatia of USC published the first journal paper on color edge detection, in which he extended the Hueckel operator, developed 4 years previously, to color images. Since then, at least 17 other journal papers and a large number of conference papers have been written.

Nearly all of them still try to "extend" a greyscale edge detector to color images. While it seems intuitive to start with the solution to an easier problem in order to attack a more complex one, there is a drawback in this particular case. We perceive grey levels to be ordered; the fact that "medium grey" and "white" can be averaged together to produce "medium-light grey" does not bother anyone. However, if you take a red and green region and try to approximate it with a single color, you will run into problems immediately. Depending on your arrangement of colors, it could be yellow (in the spectrum), grey (CIE-Lab color space), yellowish-grey (RGB, HSV) or impossible (the opponent-colors theory). Even if we could agree on the "correct" color space, none of the colors mentioned is perceptually similar to red or green. This truth is the justification of the use of color signatures.

Most of the literature can be placed into three categories: output fusion methods, multi-dimensional gradient methods, and vector methods. Output fusion appears to be the most popular; the goal is to perform edge detection three times, once each for red, green, and blue (or whatever color space is being used), and then the output is fused to form one edge map, as shown by the following diagram:

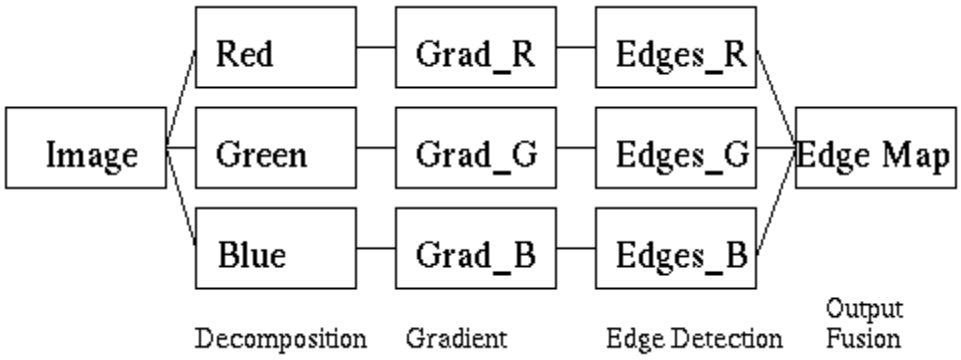


Fig 2.6: One Edge Map

Multi-dimensional gradient methods short-circuit the process somewhat by combining the three gradients into one and detecting edges only once:

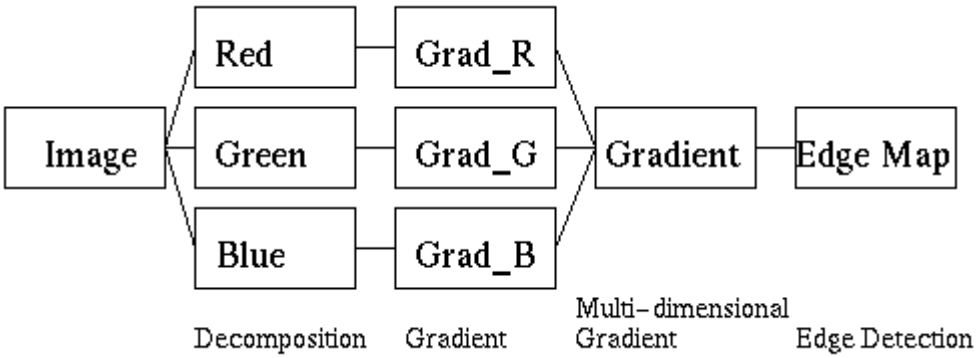


Fig 2.7: Laplacian Edge Detection

It wishes to build a morphing algorithm which operates on features extracted from target images automatically. It can be a good beginning to find the edges in the target images. Here, we have accomplished this by implementing a Laplacian Edge Detector [18].

There are many ways to perform the edge detection. However, it may be grouped into two categories that are gradient and Laplacian. The gradient method detects the edges by looking for the maximum and minimum in the first derivative of the image. The Laplacian method searches for the zero crossings in the second derivative of the image to find edges.

There are many ways to perform edge detection. However, the familiarized method can be grouped into two categories, gradient and Laplacian. The gradient method detects the edges by looking for the maximum and minimum in the first derivative of the image [18]. The Laplacian method searches for zero crossings in the second derivative of the image to find edges.

**2.6 Canny Edge Detection**

The Canny Edge Detection Algorithm has the following Steps: Step 1: Smooth the image with a Gaussian filter. Step 2: Compute the gradient magnitude and orientation using finite-difference approximations for the partial derivatives. Step 3: Apply non maxima suppression to the gradient magnitude, Use the double thresholding algorithm to detect and link edges. Canny edge detector approximates the operator that optimizes the product of signal-to-noise ratio and localization. It is generally the first derivative of a Gaussian.

The Smoothing concept has been applied in this Gaussian operation, so the finding of errors is effective by using the probability. The next advantage is improving the signal with respect to the noise ratio and this is established by Non maxima suppression method as it results in one

pixel wide ridges as the output. The third advantage is Better detection of edges especially in noise state with the help of thresholding method. The major disadvantage is the computation of Gradient calculation for generating the angle of suppression. The main disadvantage is Time consumption because of complex computation [18].

### 2.7 Close Method

In image processing, closing is, together with opening, the basic workhorse of morphological noise removal. Opening removes small objects while closing removes small holes.

### 2.8 Image Erode and Dilation

The most basic morphological operations are dilation and erosion. Dilation adds pixels to the boundaries of objects in an image, while erosion removes pixels on object boundaries. The number of pixels added or removed from the objects in an image depends on the size and shape of the *structuring element* used to process the image. In the morphological dilation and erosion operations, the state of any given pixel in the output image is determined by applying a rule to the corresponding pixel and its neighbors in the input image. The rule used to process the pixels defines the operation as a dilation or an erosion.

Image Dilation: The value of the output pixel is the *maximum* value of all the pixels in the input pixel's neighborhood. In a binary image, if any of the pixels is set to the value 1, the output pixel is set to 1.

Image Erosion: The value of the output pixel is the *minimum* value of all the pixels in the input pixel's neighborhood. In a binary image, if any of the pixels is set to 0, the output pixel is set to 0.

Morphological functions position the origin of the structuring element, its center element, over the pixel of interest in the input image. For pixels at the edge of an image, parts of the neighborhood defined by the structuring element can extend past the border of the image.

To process border pixels, the morphological functions assign a value to these undefined pixels, as if the functions had padded the image with additional rows and columns. The value of these padding pixels varies for dilation and erosion operations.

Dilation: Pixels beyond the image border are assigned the minimum value afforded by the data type. For binary images, these pixels are assumed to be set to 0. For grayscale images, the minimum value for uint8 images is 0.

Erosion: Pixels beyond the image border are assigned the *maximum* value afforded by the data type. For binary images, these pixels are assumed to be set to 1. For grayscale images, the maximum value for uint8 images is 255 [19].

The function imfill can be used to fill all holes, but this user only wanted to fill holes having an area smaller than some threshold. It can be done using a combination of imfill, bwareaopen, and MATLAB logical operators.

Window creation is used to bind a region. To find the maximum and the minimum value of the region we need to find the min max value

M = min (A) returns the smallest elements of A.

- If A is a vector, then min(A) returns the smallest element of A.
- If A is a matrix, then min(A) is a row vector containing the minimum value of each column.
- If A is a multidimensional array, then min(A) operates along the first array dimension whose size does not equal 1, treating the elements as vectors. The size of this dimension becomes 1 while the sizes of all other dimensions remain the same. If A is an empty array with first dimension 0, then min(A) returns an empty array with the same size as A.

M = max(A) returns the smallest elements of A.

- If A is a vector, then max(A) returns the smallest element of A.
- If A is a matrix, then max(A) is a row vector containing the minimum value of each column.
- If A is a multidimensional array, then max(A) operates along the first array dimension whose size does not equal 1, treating the elements as vectors. The size of this dimension becomes 1 while the sizes of all other dimensions remain the same. If A is an empty array with first dimension 0, then max(A) returns an empty array with the same size as A.

The minimum value and the maximum value will show the bounded region and it will detect the inflamed appendix.

# CHAPTER 03

# METHODOLOGY

## 3.1 Introduction

This Figure (3.2) demonstrates a block diagram of our proposed model. it shows how the algorithm is set up. After taking frames from video footage we have done pre-processing in where we have converted the RGB image into Gray image. Then we use median filtering for removing the noise and have done image binarization for edge detection. After pre processing the images we find the edges of the images by canny edge detection and we have done morphological image processing where we have used close method, erode method and hole filling method. At the end we create a window for the interested region.

### 3.2 Work flow

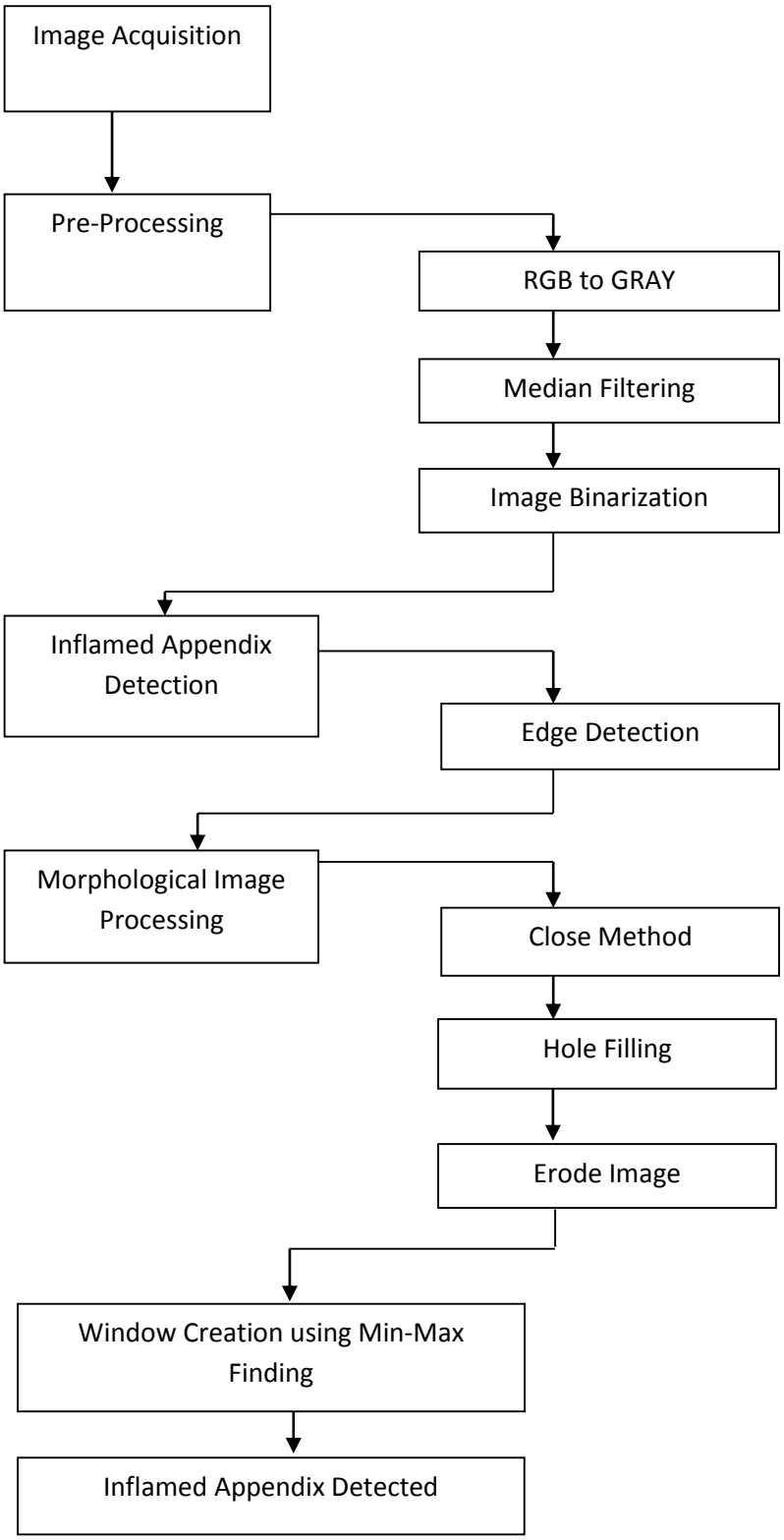


Fig 3.1: Work Flow

### 3.3 Pre processing

Preprocessing is done to clear out distortion from an image or increase some particular feature of that image for further use. Here both the input and output is intensity images. Pre-processing literally means that after applying one particular algorithm on an image the output that we get run through another algorithm and the desired result in an enhanced version of that image.

There are certain methods of preprocessing image. Such as (1) Pixel brightness, (2) Image restoration, (3) Image resolution ,(4) other methods that use local neighborhood of the processed pixel.

Image preprocessing is aimed to correct certain degradation in the image; such as correcting brightness due to the low light where the image was taken, quality improvement needed if the device has not been able to do that and for that knowledge about the acquisition device is needed.

Some of the above picture preprocessing has been used here in our proposal and they are: RGB to Grayscale, Median filtering and image binarization. Image preprocessing methods use the considerable redundancy in an image.

TV cameras or some other high definition video cameras have automatic system that helps to work under unstable illumination condition. Laparoscopic video capturing camera cannot have that due to limitation of being used inside the human body and that is why preprocessing is needed to be done on the images produced by it.

Fig 3.2: Image from Laparoscopic video footage for preprocessing

### 3.3.1 RGB to Grayscale

We perceive color through wavelength-sensitive sensory cells called cones which are three different types of cones, each with a different sensitivity to electromagnetic radiation (light) of different wavelength. One is sensitive to red light, one to green light, and one to blue light. By emitting a controlled combination of these three basic colors (red, green and blue), and hence stimulate the three types of cones at will, we are able to generate almost any perceivable color. This is the reasoning behind why color images are often stored as three separate image matrices; one storing the amount of red (R) in each pixel, one the amount of green (G) and one the amount of blue (B). We call such color images as stored in an RGB format.

In grayscale images, however, we do not differentiate how much we emit of the different colors; we emit the same amount in each channel. What we can differentiate is the total amount of emitted light for each pixel; little light gives dark pixels and much light is perceived as bright pixels.

Converting RGB to grayscale, we have to take the RGB values for each pixel and make as output a single value reflecting the brightness of that pixel. One such approach is to take the average of the contribution from each channel: (R+B+C)/3.That is what the tool that we use basically does. But the important question here is why we need gray scaling in our project? Well the answer to do this is to get the correct signal of noise. For many applications of image processing, color information doesn't help us identify important edges or other features. There are exceptions. If there is an edge (a step change in pixel value) in hue that is hard to detect in a grayscale image, or if we need to identify objects of known hue (orange fruit in front of green leaves), then color information could be useful. If we don't need color, then we can consider it noise. At first it's a bit counterintuitive to "think" in grayscale, but you get used to it.

Secondly for an easier code. It is hard to find the correct edges in a colored image and so the result is highly depressive and complex code extensions are needed to find them and also the efficiency isn’t satisfying. Gray scaling doesn’t have any additional color information that has to be stored and worked on making code easier with practically high efficiency.

The lightness method averages the most prominent and least prominent colors: (max(R, G, B) + min(R, G, B)) / 2.The formula for luminosity is 0.21 R + 0.72 G + 0.07 B.

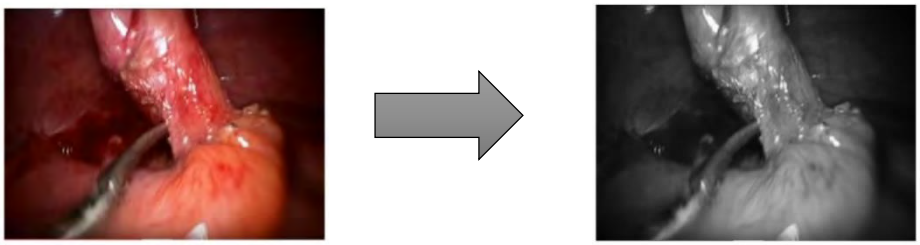

Fig 3.3(a): RGB

Fig 3.3(b): RGB to Gray scale

The figure above represents the transformation from RGB to gray scale image.

### 3.3.2 Median Filtering

The previous processing done to the image can suppress isolated out-of-range noise, but the side effect is that it also blurs sudden changes such as line features, sharp edges, and other image details all corresponding to high spatial frequencies.

The median filter is an effective method that can, recognize out-of-range isolated noise from legitimate image features such as edges and lines. Specifically, the median filter replaces a pixel by the median, instead of the average. So we considered a group of non linear filters that has a output of linear combination in a particular image of the inflamed appendicitis. If we assume that the white noise with signal of linear constant is used to minimize the mean square error. There is a number of algorthin that exist to help doing the median filtering with lowest complexity of 0( n^2).

Impulse noise reduction algorithms can be classified in to two classes: linear and nonlinear algorithms. Many image de-noising algorithms for correcting the images corrupted by impulse noise. In a linear technique, the noise reduction method is applied linearly to all the pixels in the input image without checking for the corrupted pixels, whereas in non-linear methods corrupted and no corrupted pixels are determined first then the reduction techniques are applied for correcting the corrupted pixels only.

The image that we got from the Laparoscopy footage had been median filtered to distinguish the inflamed appendicitis and for that the edge has to recognize correctly. Every single pixel has its own importance and none can be left out or else that could point to a different object

and add great risk to patient's health. We have used the following equation for filtering the image.

$$y[m,n] = median\{x[i,j], (i,j) \in w\} \quad (1)$$

where w represents a neighborhood defined by the user, centered around location [m,n] in the image.

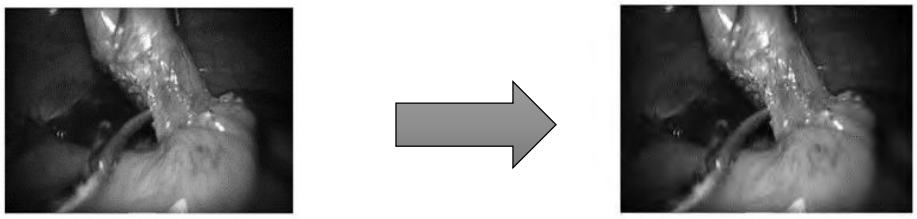

Fig 3.4(a): Gray scale

Fig 3.4(b): Gray scale to Median filtered

The Figures above represents the formation from gray scale to median filtering.

### 3.3.3 Image Binarization

Binarization is the process of converting a pixel image into binary image. It is the basis of segmentation. After converting the image that we got from the Laparoscopic footage to gray scale a threshold is applied. This applied threshold can be fixed or be depending on clustering algorithm. A wrong selection of threshold value may misinterpret the background pixel and can classify it as object and vice versa, resulting in overall degradation of whole surgical performance. Binarization is mainly needed for the recognition of the object and in this case it is the inflamed appendicitis. The part of the abdomen where the surgery will take place will have many layers and surrounding objects. We had to differentiate the appendicitis from them. Finding the depth and exact position of it.

Proper Binarization is very important to differentiate the foreground object from the background. Binarization can be very challenging if done on noisy mages and so it is very important to remove the noise at first and that is why we have done Binarization the image at the last stage of preprocessing. The majority of binarization techniques are complex and are compounded from filters and existing operations. However, the few simple thresholding methods available cannot be applied to many binarization problems. We have used the equation below for thresholding and further binarizing the image.

$$P(C_j|x) = \frac{|\Sigma_j\llbracket \quad |(t)|\rrbracket\hat{}(-1/2)\ e\hat{}(n\_j\ )\ P\_j\ (t)}{\sum_{k=1}^{M}|\sum_j(t)|e^{-\frac{1}{2}e^{n_j}P_k(t)}} \tag{2}$$

The above equation is for the thresholding of binarization , where where 'cj' is the is the value of the pixel after binarization.the denominator is the average of all pixel of the image before binarization and numerator is the average pixel before binarization.

### 3.4 Edge Detection

Edge detection is an image processing technique by which we can found the boundaries of objects within images. It works by counting the discontinuities in the brightness. It is used for image segmentation and data extraction in areas such as image processing, computer vision and in machine vision. Some of the common edge detection techniques are Canny, Sobel, Prewitt, Roberts and fuzzy logic method. We use canny edge detection for our work.

#### 3.4.1 Canny Edge Detection

Canny edge detection is a multi-step algorithm that can detect edges with noise suppressed at the same time. The process of canny edge detection algorithm can be broken into five different steps: Gaussian filtering, finding intensity gradient, non maxima suppression and hysteresis thresholding. Since all edge detection results are easily affected by image noise, it is essential to filter out the noise to prevent false detection caused by noise. To smooth the image, a Gaussian filter is applied to convolve with the image The equation (i) is for a Gaussian filter kernel of size $(2k+1) \times (2k+1)$ is given by:

$$H_{ij} = \frac{1}{2\pi\sigma^2}\exp\left(-\frac{(i-(k+1))^2+(j-(k+1))^2}{2\sigma^2}\right);\ 11 \le i,j \le (2k+1) \tag{3}$$

Here is an example of 5*5 Gaussian Filter, used to create the adjacent image with $\sigma = 1{,}4$

$$B = \frac{1}{159}\begin{bmatrix} 2 & 4 & 5 & 4 & 2 \\ 4 & 9 & 12 & 9 & 4 \\ 5 & 12 & 15 & 12 & 5 \\ 4 & 9 & 12 & 9 & 4 \\ 2 & 4 & 5 & 4 & 2 \end{bmatrix} * A.$$

After the Gaussian filtering we can find edge gradient and direction for each pixel as follows:

$$G = \sqrt{G_x^2 + G_y^2} \tag{4}$$

$$\text{Angle}(\theta) = \tan^{-1}\left(\frac{G_y}{G_x}\right) \tag{5}$$

After getting gradient magnitude and direction, a full scan of image is done to remove any unwanted pixels which may not constitute the edge. For this, at every pixel, pixel is checked if it is a local maximum in its neighborhood in the direction of gradient. Then we do hysteresis thresholding for getting the information which are the real edge. For this, we need two threshold values, minVal and maxVal. Any edges with intensity gradient more than maxVal are sure to be edges and those below minVal are sure to be non-edges, so discarded. Those who lie between these two thresholds are classified edges or non-edges based on their connectivity. If they are connected to "sure-edge" pixels, they are considered to be part of edges.

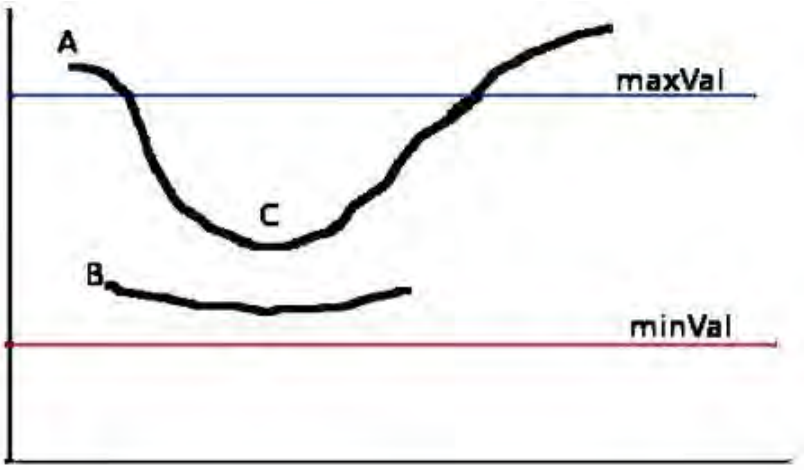


Fig 3.5: The edge A is above the maxVal, so considered as "sure-edge". Although edge C is below maxVal, it is connected to edge A, so that also considered as valid edge and we get that full curve. But edge B, although it is above minVal and is in same region as that of edge C, it is not connected to any "sure-edge", so that is discarded.

As canny edge can detect the sharp edges it is useful for medical images to detect the region because in medical images there are too many neighbor edges and it is sometimes tough to detect the region if we cannot get the proper edges. We use canny edge detection because for medical image it is more efficient. In canny edge detection at first the Gaussian filtering is being processed then we analyze the value of X-axis and Y-axis and set the parameter of the radius value to 10. Previously we have done median filtering for removing the noise. Figure show below determines the conversion from median filtering to canny edge detection

Fig 3.6(a): Median filtered image

Fig 3.6(b): Canny edge detected images

### 3.5 Morphological Image Processing

The word morphology commonly denotes biological term which deals with the form of structure of plant and animal. In mathematical Image processing we use morphological as a tool for extracting image components that are useful to represent the region shape.

Morphological techniques probe an image with a small shape or template called structural element. This structural element is a binary image which is represented by matrix. The matrix dimension specifies the size of the structure element. The pattern of ones and zeros specify the structure element.

#### 3.5.1 Close method

Closing is an important operator in mathematical morphology. It is normally applied to binary images. The closing operator needs two inputs: an image to be closed and a structuring element. Close method is basically a combination of dilation and erosion.

#### 3.5.2 Dilation and Erosion

Erode is the one of the two basic operation of morphological image processing. It is applied to the binary image. The basic effect of the operator on a binary image is to erode away the boundaries of regions of pixels. Thus area of foreground of pixels shrink in size and holes within area become larger. Another basic operation is Dilation. It is also applied to binary images. For dilation the basic effect of an operator is the gradually enlarge the boundaries of the regions od foreground pixels. So in general we can say dilation causes objects to grow or dilate in image and erosion causes to shrink the image. Dilation and Erosion is defined by following:

$$\text{Dilation: } D(A,B) = \bigcup_{\beta \epsilon B} Y(A+\beta) \tag{6}$$

$$\text{Erosion: } E(A,B) = \bigcup_{\beta \epsilon B} Y(A-\beta) \tag{7}$$

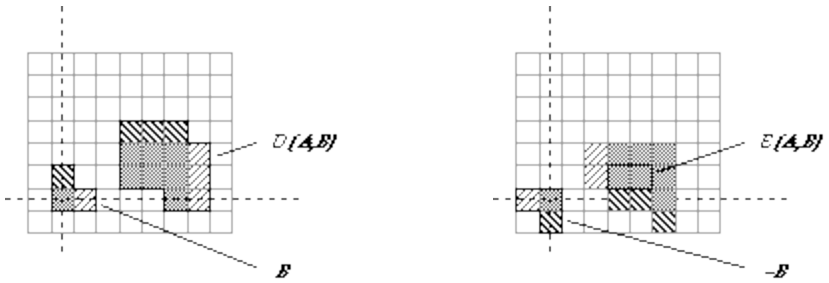


Fig 3.7: Dilation and Erosion

A binary image containing two object sets *A* and *B*. The three pixels in *B* are "color-coded" as is their effect in the result.

While either set *A* or *B* can be thought of as an "image", *A* is usually considered as the image and *B* is called a structuring element.

As we want to detect the region of an organ we need to close some area for getting our resulting image. So we use close method for filling the gaps between the edges and smoothed the outer edges. To do this we need to dilate the image first and then erode the image. To dilate the gray scale image we perform vector addition of set elements. When we dilate the images the we get more sharp images because we perform union operation with the neighbor value of the gray scale image and thus the difference between the edge and the and the background is increased which helps us to detect the region more accurately after this we do the erosion process which we will discuss later in the erosion part.

Fig 3.8(a): Canny edge detected image

Fig 3.8(b): Close Image

The Figures above shows the conversion of canny edge detection to close image.

### 3.5.3 Hole Filling

Hole Filling is kind of Flood Fill algorithm. It is used for filling image regions and holes. The algorithm looks for all nodes in the array that are connected to the start node by a path of the target color and changes them to the replacement color. Mathematical representation of region filling is:

$$X_k = (X_{k-1} \oplus B) \cap A^c \qquad k = 1,2.3 \dots \dots \dots \tag{8}$$

where A denotes a set whose elements boundary points of a region B is the semantic structural element. the algorithm stops if $X_k = X_{k-1}$. The set union of $X_k$ and A contains the filled set and its boundary.

In our work we use hole filling to fill the holes in the interested region. Before doing hole filling we close the image after that to fill the hole we measure the value of X-axis and the value of Y-axis. Then we scan the values of rows and columns and get the coordinates of the close image. Then we set the value to 0 except for the region of interest and the other all value set to 1. After this we convert the region of interest into RGB image.

Fig 3.9(a): Close Image

Fig 3.9(b): Hole filled image

The Figures above determines the conversion of close image to hole filled image.

We mapped holed fill image to RGB image to see what types of output comes. The figures below show the conversion of holed filled image and holed filled image mapping into RGB image.

Fig 3.10(a): hole filled image

Fig 3.10(b): holed filled image mapped to RGB

### 3.5.4 Erosion

After dilation we erode the resulting image. In erosion we perform vector subtraction of set elements. After eroding the image we get thinner edge as we perform subtraction methods between the region and its neighbor value. Thus we get more precious image of the region we are working on.

After second time erosion we get the below images then mapped the images to RGB images.

Fig 3.11(a): Eroded Image

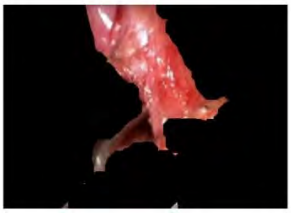

Fig 3.11(b): Eroded image mapped to RGB image

### 3.6 Min-Max for window Creation

Window creation is a process by which a region is bounded. For this bounding option we measure the value of the region of interest. After this we get the value of $X_{min}, X_{max}, Y_{min} and\ Y_{max}$ . From these we measure the difference between the maximum and minimum value of X axis and Y axis. Then we create a window with a width of this difference value and mapped the whole image into RGB image.

$$diff(x) = X\_axis_{max} - X\_axis_{min} \quad (9)$$

$$diff(y) = Y\_axis_{max} - Y\_axis_{min} \quad (10)$$

$$\text{Window width and length} = diff(x,y) \quad (11)$$

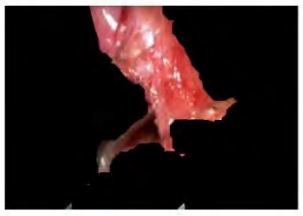

Fig 3.12(a): Eroded image (RGB)

Fig 3.12(b): Window Creation

The Figure above shows that we have got our region of interest which is shown in Fig 3.11(a) and after that in the Fig 3.11(b) we see that that region is bounded by a window which was our target.

# CHAPTER 04

# EXPERIMENTAL ANALYSIS

## 4.1 Introduction

Flow work showed in chapter 3.2 demonstrates a detailed implementation of our proposed model. It demonstrates how the algorithm is set up.

## 4.2 Using Erosion again

In our setup we use erosion method for the second time after it is being applied in the close method which is combined of erosion and dilation. After detecting the edges we use close method.

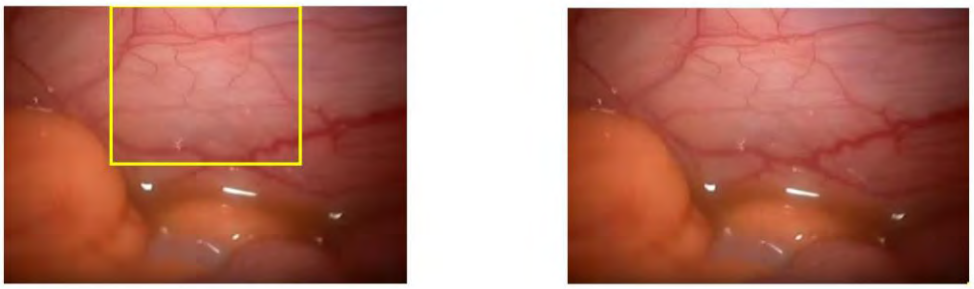

Fig 4.1: Differece after first time eroding and second time eroding

After closing method we get the first image of Figure. In this image we can see that a window is created as there is a region of interest where there is no region of interest. So we do second time erosion and convert the eroded image into RGB image which is shown in the second image of the figure. In this there is no window as there is no region of interest.

### 4.3 Changes in the Accuracy Rate based on the changes in Threshold Values

Table 1: Accuracy rate based on threshold value from 0.1 to 0.9

| Threshold value | Detected ROI | Accuracy |
|---|---|---|
| **0.1** | **13** | **54.17%** |
| **0.2** | **12** | **50.00%** |
| **0.3** | **10** | **41.67%** |
| **0.4** | **6** | **25.00%** |
| **0.5** | **2** | **8.34%** |
| **0.6** | **1** | **4.16%** |
| **0.7** | **0** | **0.00%** |
| **0.8** | **0** | **0.00%** |
| **0.9** | **0** | **0.00%** |

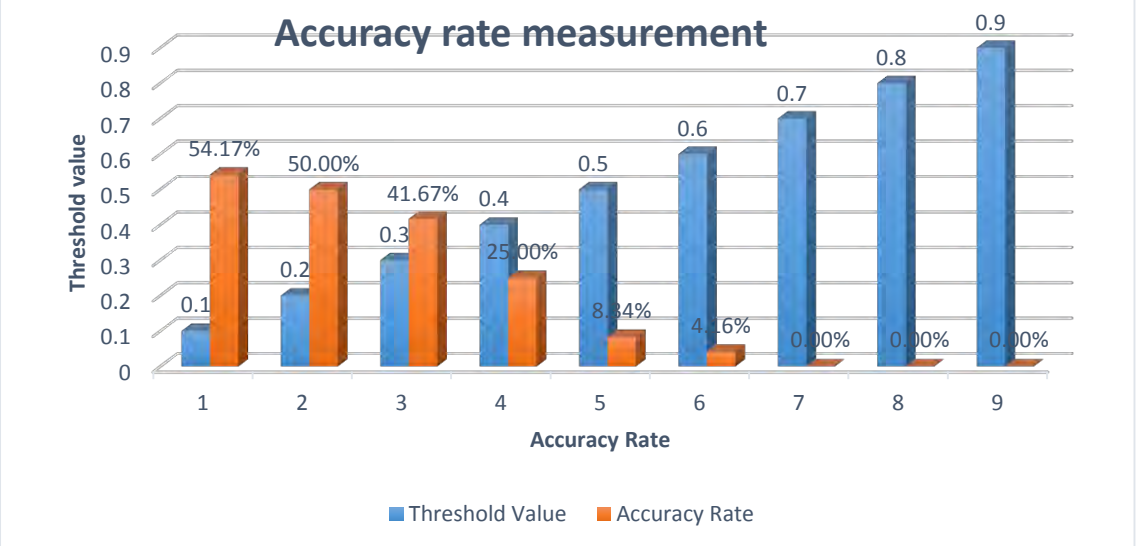


Fig 4.2: Accuracy rate based on threshold value from 0.1 to 0.9

From the graph we see that when the threshold value is 0.1 the accuracy is good when the value is 0.2 it is less than the value of 0. 1 .We sees that the value is gradually decreasing from the threshold value 0.2 to 0 .9. So we will set the threshold value between 0.1 to 0.2.

Table 2: Accuracy rate based on threshold value from .11 to .19

| Threshold Value | Detected Image | Accuracy |
|---|---|---|
| .11 | 16 | 66.67% |
| .12 | 20 | 83.33% |
| .13 | 17 | 70.83% |
| .14 | 16 | 66.67% |
| .15 | 16 | 66.67% |
| .16 | 18 | 75.00% |
| .17 | 19 | 79.16% |
| .18 | 17 | 70.83% |
| .19 | 13 | 54.16% |

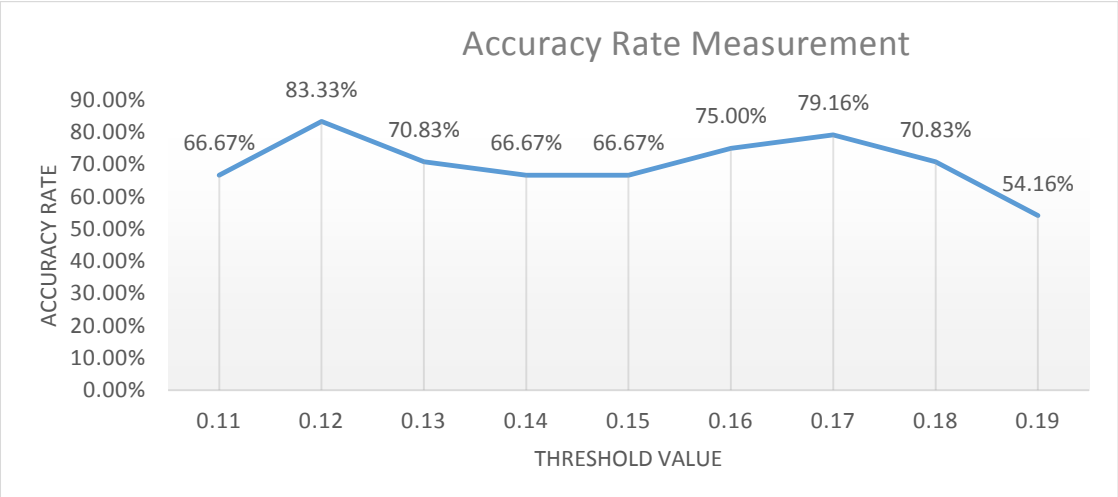


Fig 4.3: Accuracy rate based on threshold value

From this Graph 2 we see that the accuracy level is highest when the threshold value is 0.12. At the threshold level 0.12 the accuracy is 82.33% which is good enough to detect the inflamed appendix.

# CHAPTER 05

# CONCLUSIONS AND FUTURE WORKS

## 5.1 Concluding remarks

In this thesis paper which is based on the experimental result shows a new approach to image processing from Laparoscopic video footage using edge detection and morphological image processing. We have proposed a new idea of acquiring processed image for detecting an inflamed appendix. With the help of this idea surgery will be more efficient and easier. Our results have shown an excellent accuracy percentage leading to a new branch of automatic surgery system. In the 0.12 threshold value the accuracy rate is 83.33%.

Day by day new ideas are arriving and we believe future works will bring more efficiency in the field of medical science. We are hopeful that our idea will contribute to the surgical world and bring betterment to the society.

## 5.2 Future Works

In this study we have worked on inflamed appendix detection from laparoscopic video where we used edge detection and morphological image processing technique. The potential future directions for research based on the results presented in this thesis can be characterized into the following sections.

### 5.2.1 Work for detection on other organs

Using laparoscopy to find problems such as cysts, adhesions, fibroids, and infection. Tissue samples can be taken for biopsy through the tube.

### 5.2.2 Robotic Surgery

Laparoscopic operations are done manually. In future we will work to increase the efficiency of the robot to do the operation automatically

# REFERENCES

[1] Williams NM, Jackson D, Everson NW, Johnstone JM (1998)

[2] Delibegovic S, Iljazovi E, Katica M, Koluh A (2011) Tissue reaction to absorbable endoloop, nonabsorbable titanium staples, and polymer Hem-o-lok clip after laparoscopic appendectomy.JSLS 15: 70-76

[3] Delibegovic S, Katica M, LatiÄ‡ F, JakiÄ‡-RazumoviÄ‡ J, Koluh A, et al. (2013) Biocompatibility and adhesion formation of different endoloop ligatures in securing the base of the appendix.JSLS 17: 543-548.

[4] Gagner M, Garcia-Ruiz A (1998) Technical aspects of minimally invasive abdominal surgery performed with needlescopic instruments.Surg Laparosc Endosc 8: 171-179.

[5] Schier F (1998) Laparoscopic appendectomy with 1.7-mm instruments.Pediatr Surg Int 14: 142-143.

[6] Panait L, Bell RL, Duffy AJ, Roberts KE (2009) Two-port laparoscopic appendectomy: minimizing the minimally invasive approach.J Surg Res 153: 167-171.

[7] Rispoli G, Armellino MF, Esposito C (2002) One-trocar appendectomy.Surg Endosc 16: 833-835.

[8] Deie K, Uchida H, Kawashima H, Tanaka Y, Masuko T, et al. (2013) Single-incision laparoscopic-assisted appendectomy in children: exteriorization of the appendix is a key component of a simple and cost-effective surgical technique. Pediatr Surg Int29:1187-1191.

[9] St Peter SD, Adibe OO, Juang D, Sharp SW, Garey CL, et al. (2011) Single incision versus standard 3-port laparoscopic appendectomy: a prospective randomized trial.Ann Surg 254: 586-590.

[10] Teoh AY, Chiu PW, Wong TC, Wong SK, Lai PB, et al. (2011) A case-controlled comparison of single-site access versus conventional three-port laparoscopic appendectomy.Surg Endosc 25: 1415-1419.

[11] Kum CK, Ngoi SS, Goh PM, Tekant Y, Isaac JR (1993) Randomized controlled trial comparing laparoscopic and open appendicectomy.Br J Surg 80: 1599-1600.

[12] Oddsdottir M, Hunter JG (1995) Laparoscopic approach to suspected appendicitis. In: Arregui ME, Sackier JM. Eds. Minimal access coloproctology. Radcliffe Medical Press. Oxford and New York 103-121.

[13] Andersson RE, Schein M (2012) Antibiotics as first-line therapy for acute appendicitis: evidence for a change in clinical practice.World J Surg 36: 2037-2038.

[14] Smith AG, Ripepi A, Stahlfeld KR (2002) Case report. Retained fecalith. Laparoscopic removal. Surgical Laparoscopy; Endoscopy and percutaneous techniques 12:441-442.

[15] Tzovaras G, Liakou P, Baloyiannis I, Spyridakis M, Mantzos F, et al. (2007) Laparoscopic appendectomy: differences between male and female patients with suspected acute appendicitis.World J Surg 31: 409-413.

[16] Neudecker J, Sauerland S, Neugebauer EAM, Bergamaschi R, Bonjer HJ, et al. (2006) The EAES clincial practice guidelines on the pneumoperitoenum for laparoscopic surgery (2002). In: EAES guidelines for endoscopic surgery. Eds. Neugebauer EAM, Sauerland S, Fingerhut A, Millat B, Buess G. Springer39-85.

[17] Addiss DG, Shaffer N, Fowler BS, Tauxe RV (1990) The epidemiology of appendicitis and appendectomy in the United States.Am J Epidemiol 132: 910-925.

[18] Canny, J., “A Computational Approach to Edge Detection”, IEEE Trans. Pattern Analysis and Machine Intelligence, vol. 8:679-714, November 1986.

[19] R. C. Gonzalez and R. E. Woods, Digital image processing, 2nd ed. Upper Saddle River, N.J.: Prentice Hall, 2002.